Structural Transformation of Boron Nitride Nanoparticles in Benzene under Moderate Conditions

Zefeng Lai[a,b], Lingling Zhu[a], Lili Yu[a], Zhi Chen[a,b], Xian Zhao[a], Qilong Wang[b],
Deliang Cui[a], and Minhua Jiang[a]

[a] State Key Lab of Crystal Materials, Shandong University, Jinan 25 0100, P. R. China
[b] School of Chemistry & Chemical Engineering, Shandong University, Jinan 250100, P. R. China

Reprint requests to Prof. Dr. De-Liang Cui. Fax: +86-531-88361856. E-mail: cuidl@sdu.edu.cn

Z. Naturforsch. **61b,** 1555 – 1560 (2006); received July 13, 2006

This work reports a new route for preparing cubic BN (*c*-BN) nanocrystals under moderate conditions. Considering the instability of BN nanoparticles, we have investigated the structural transformation of BN nanoparticles in benzene. The results revealed that a great deal of hexagonal BN (*h*-BN) nanoparticles had been converted into *c*-BN or wurtzitic BN (*w*-BN) at 280 °C and 50 MPa. As the temperature was increased from 280 to 300 °C, *h*-BN nanoparticles gradually disappeared, and the content of both *c*-BN or *w*-BN increased. Similarly, increase of pressure or hot-pressing time showed the same effect. These results may open up an opportunity for synthesizing other superhard nanomaterials such as diamond and cubic carbon nitride under moderate conditions.

Key words: Boron Nitride Nanoparticles, Solvent Hot-pressing Route, Structural Transformation, Characterization

Introduction

As a superhard material, cubic boron nitride (*c*-BN) has many excellent merits, for example, superhardness (∼ 47 GPa, only inferior to diamond), high thermal stability, high thermal conductivity, inertness to ferrous materials and wide band gaps (∼ 6.4 eV) *etc.* [1 – 3]. These merits make *c*-BN an ideal candidate for the fabrication of cutting tools, high power electronic devices, ultraviolet light emitting devices and detectors *etc.* [4, 5]. Therefore, *c*-BN has attracted much attention since the first successful synthesis at high temperature (1800 °C) and under high pressure (8.5 GPa) in 1957 [6]. In order to prepare this material under moderate conditions, many kinds of alkaline and alkaline earth metal nitrides were used as catalysts [7 – 14]. Kobayashi [15] synthesized *c*-BN under relatively moderate conditions by using water, urea and boric acid as catalysts. Takashi [16] accomplished the transformation from *h*-BN to *c*-BN at lower temperature and pressure by adding some water.

Recent results indicated that both temperature and pressure could be drastically decreased when amorphous BN or BN nanoparticles were used as the starting materials for the transformation [16, 17]. We have investigated the solid state structural transformation of BN nanoparticles under moderate conditions, and found that part of orthorhombic BN (*o*-BN) [18] and *h*-BN nanoparticles could be converted into *c*-BN at 270 – 325 °C and 0.6 – 0.9 GPa [19]. Besides, we have also noticed that the small BN nuclei dispersed in solvothermal solutions might be partly converted into *c*-BN or wurtzitic BN (*w*-BN, a sp^3 hybrid modification of BN with a two-layered stacking sequence (ABAB. . .), the structure of which is analogous to hexagonal diamond [20, 21]) at 280 – 300 °C and 6 – 10 MPa. All this work suggested that BN nanoparticles might be converted into *c*-BN or *w*-BN at much lower temperature and pressure when they were dispersed in a liquid medium. On the basis of this idea, we have devoted much effort to exploring the structural transformation from *h*-BN nanoparticles to *c*-BN in benzene. To the best of our knowledge, such results have never been reported by other researchers before. It is believed that this result will be of great importance and facilitate the preparation of larger amounts of *c*-BN nanoparticles.

Results and Discussion

Characterization of the starting material

X. P. Hao *et al.* have successfully synthesized *c*-BN nanocrystals by the benzene solvothermal synthesis method, however, *o*-BN, *c*-BN and *h*-BN coexist in the samples [22]. Using the solvothermal method for syn-

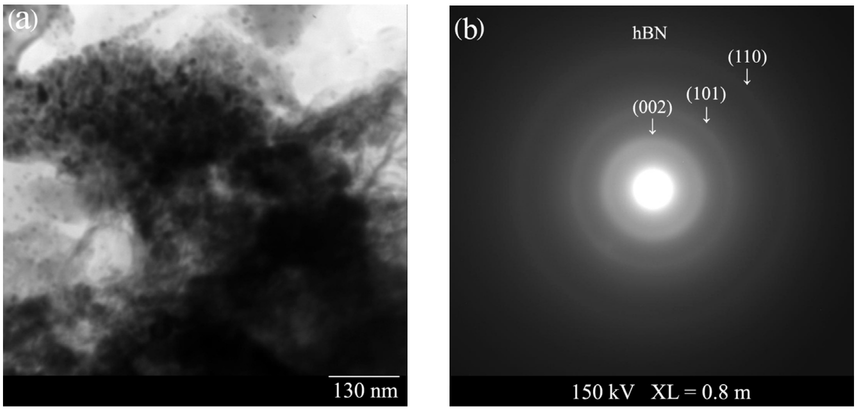

Fig. 1. TEM image and SAED pattern of the starting material. (a) coagulated *h*-BN nanoparticles, (b) the corresponding SAED pattern.

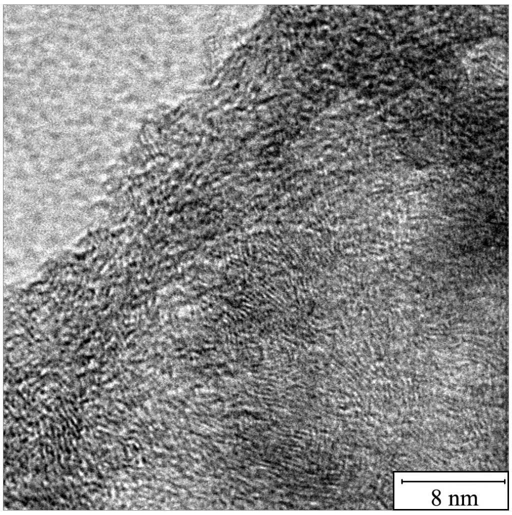

Fig. 2. An HRTEM image of the starting material.

thesizing pure *c*-BN, we found that *h*-BN and *c*-BN nanoparticles transform into each other in a reversible way, *i. e.* *h*-BN nanoparticles transformed into *c*-BN when the temperature and pressure were increased, and the reverse transformation from *c*-BN nanoparticles to *h*-BN took place with decreasing temperature and pressure at the end of the experiment. As a result, a large amount of *h*-BN nanoparticles appeared in the samples.

As is shown in Fig. 1, the samples prepared by the benzene solvothermal method mainly contain coagulated *h*-BN nanoparticles with an average particle size of ~ 8 nm. Fig. 2 shows an HRTEM image taken from the sample which is mainly composed of poorly crystallized *h*-BN nanoparticles. Fig. 3(a) shows the corresponding IR absorption spectrum of the starting material. In this spectrum, the strong broad band at 1387 cm^{-1} can be attributed to the B–N tensile vibrations of *h*-BN [23]. Comparatively, the peak at $\sim 1070\ \text{cm}^{-1}$ which is the characteristic TO mode absorption of *c*-BN [2, 23] is rather weak. The analysis suggests that the main product of the reaction between BCl_3 and NaN_3 under the above mentioned conditions should be *h*-BN. The peak at 1629 cm^{-1} arises from adsorbed H_2O in the sample.

Phase transformations of BN in benzene

We have found that poorly crystallized *h*-BN nanoparticles can be converted into *c*-BN or *w*-BN under much milder conditions, compared to those needed for the phase transformation from crystalline *h*-BN. This may be due to the instability of the nanoparticles. It is reported that the medium around nanoparticles plays an important role in determining the interface energy, which in turn affects the stability of nanoparticles [24]. The phase transformation from amorphous *h*-BN to *c*-BN promoted by adding some water to the *h*-BN [16] may serve as evidence for this opinion.

The effect of temperature on the structural transformation

Previous studies have proven that a critical temperature may exist for the structural transformation from *h*-BN nanoparticles to *c*-BN [25, 26]. This also holds for our experiments. FTIR spectra of BN samples prepared at different temperatures from the starting material are shown in Fig. 3. By comparing spectra (a) and (b), it is hard to find any change after the starting material was hot-pressed at 240 °C, because the characteristic peaks of *c*-BN ($\sim 1047\ \text{cm}^{-1}$) and *w*-BN ($\sim 1085\ \text{cm}^{-1}$) [2] are nearly unobserv-

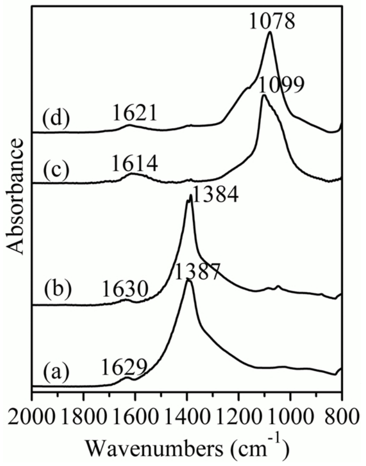

Fig. 3. FTIR absorption spectra of BN samples. (a) The starting material; (b) 240 °C, 120 MPa, 6 h; (c) 280 °C, 120 MPa, 6 h; (d) 300 °C, 120 MPa, 6 h.

able. As the temperature is further increased to 280 °C, the strong band at 1384 cm^{-1}, which is characteristic of *h*-BN, disappears while a strong and broad band around 1000 – 1200 cm^{-1} emerges. This indicates that almost all of the *h*-BN nanoparticles have transformed into *c*-BN or *w*-BN at this temperature. This result reveals that 280 °C may be a critical temperature for the structural transformation of BN nanoparticles.

Fig. 4 shows the results obtained by a multi-peak Lorentzian fitting method. In Fig. 4(a), the ratio of the peak area of *c*-BN (at 1054 cm^{-1}) to that of *w*-BN (at 1102 cm^{-1}) is 1.8 : 1.0. This ratio increases to 2.1 : 1.0 in Fig. 4(b), revealing that the content of *c*-BN increased with the increase of the hot-pressing temperature.

Besides the increase of the contents of *c*-BN or *w*-BN, the crystalline perfection of the samples has

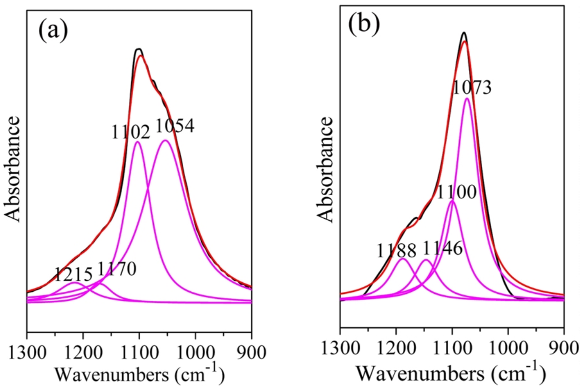

Fig. 4. Fitting results of the FTIR bands of BN samples. (a) The fitting result of the band in Fig. 3(c); (b) the fitting result of the band in Fig. 3(d). The peaks at 1054 – 1073 cm^{-1} are attributed to *c*-BN, and those at 1100 – 1102 cm^{-1}, 1146 – 1170 cm^{-1}, and 1188 – 1215 cm^{-1} to *w*-BN. (The Origin Pro 7.0 software was used in the analysis of the bands of Fig. 3(c) and (d)).

also been improved by hot-pressing treatment. Fig. 5 shows the morphology and selective area electron diffraction (SAED) pattern of some nanocrystals in the sample prepared by hot-pressing at 300 °C, indicating that many nanocrystals in cubic shape were formed. The SAED pattern confirms that the cubic-shaped nanocrystals are *c*-BN. Evidently, the crystalline perfection of the sample is improved very much, compared to that of the starting materials (see Fig. 1).

The effect of pressure on the structural transformation

The above results have revealed that 280 °C is to be taken as a critical temperature for the structural transformation of BN nanoparticles. Fig. 6 presents a comparison between the FTIR spectra of the starting material and those of samples prepared by hot-pressing at

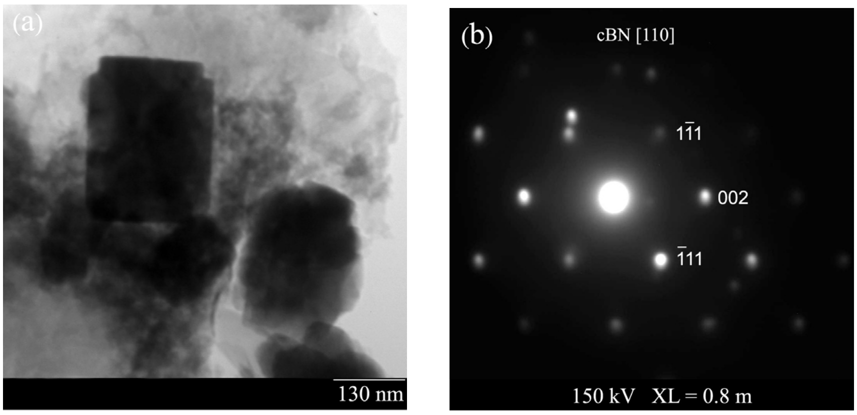

Fig. 5. TEM image and SAED pattern of *c*-BN nanocrystals. The sample was prepared by hot-pressing the starting material at 300 °C and 120 MPa, the spots in (b) can be indexed to the (1 1 1), (002) and (1 11) diffractions of *c*-BN.

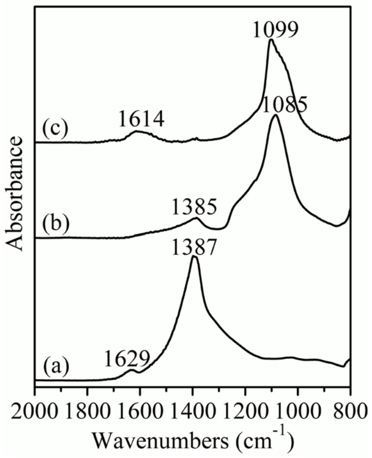

Fig. 6. FTIR absorption spectra of samples prepared at different pressures. (a) Starting material; (b) 280 °C, 50 MPa, 6 h; (c) 280 °C, 120 MPa, 6 h.

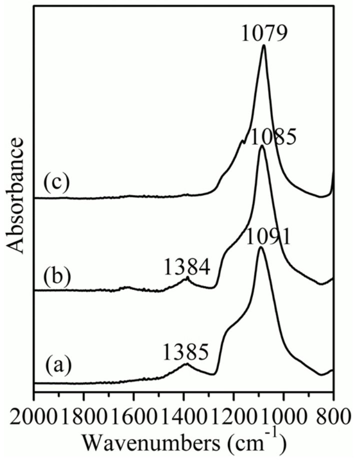

Fig. 7. FTIR absorption spectra of the samples hot-pressed for different periods of time. (a) 280 °C, 83 MPa, 1 h; (b) 280 °C; 83 MPa, 2 h; (c) 280 °C, 83 MPa, 4 h.

the same temperature (280 °C) but under different pressures. It can be seen that *h*-BN nearly disappeared, and that *c*-BN or *w*-BN became the major phases after being hot-pressed at 280 °C and 50 MPa. According to Figs. 6(a), (b) and (c), the ratios of the contents of *h*-BN, *c*-BN and *w*-BN are 1.0 : 0 : 0, 0.14 : 0.83 : 1.0 and 0 : 1.8 : 1.0, respectively. It may be concluded that pressure has an obvious effect on the relative contents of *c*-BN or *w*-BN at the critical temperature.

The effect of hot-pressing time on the structural transformation

The hot-pressing time also plays an important role in the amount of *c*-BN and *w*-BN formed. In order to investigate its effects on the structural transformation of BN nanoparticles, we have conducted experiments under 83 MPa at 280 °C (the critical temperature for the structural transformation of BN nanoparticles), where the hot-pressing time varied from 1 h to 2 h and 4 h. The FTIR spectra of the samples thus prepared are shown in Fig. 7. It is obvious that the peak at ~ 1384 cm^{-1}, which is characteristic of *h*-BN, gradually disappears with prolonged hot-pressing time. At the same time, a shift of the strongest peak from 1091 to 1087 and 1079 cm^{-1} occurs, revealing that the content of *c*-BN increased with prolonged hot-pressing time. This is supported by the fitting results of the FTIR spectra (Fig. 8). From Fig. 8, it can be calculated that the ratios of the contents of *h*-BN : *c*-BN : *w*-BN are 0.27 : 0.49 : 1.0, 0.05 : 0.48 : 1.0 and 0 : 1.13 : 1.0, corresponding to the samples hot-pressed for 1 h, 2 h and 4 h, respectively.

Conclusions

The structural transformation of BN nanoparticles at reduced temperature and pressure is mainly due to

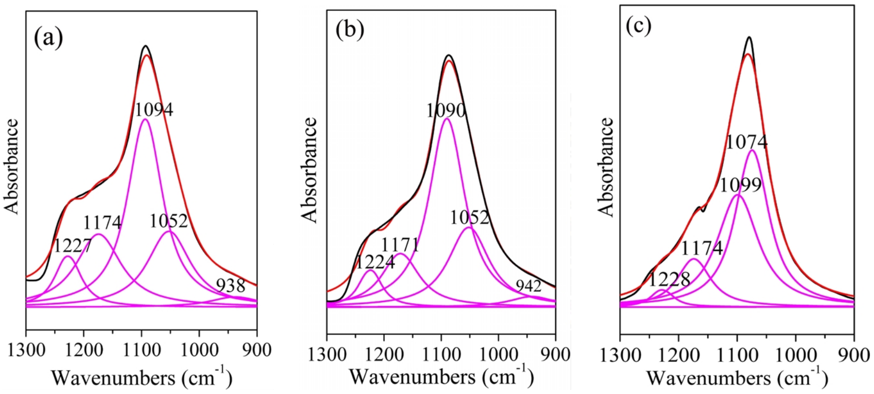

Fig. 8. Fitting results of the FTIR bands in Fig. 7. Figs. 8(a), (b) and (c) are corresponding to Figs. 7(a), (b) and (c), respectively. The peaks at 1052 – 1074 cm^{-1} can be attributed to *c*-BN, those at 1090 – 1099 cm^{-1}, 1171 – 1174 cm^{-1} and 1224 – 1228 cm^{-1} to *w*-BN.

their high surface energy and instability. In addition, a liquid environment can further facilitate such a structural transformation under moderate conditions. Our research has shown that *h*-BN nanoparticles can be converted into *c*-BN or *w*-BN under rather moderate conditions. The ratio of the contents of *c*-BN to *w*-BN increases with increasing temperature, pressure and time, and 280 °C is the critical temperature for the transformation of BN nanoparticles. Although BN nanoparticles have not been completely converted into *c*-BN in our experiments, it can be expected that the solvent hot-pressing route will continue to give better results pertaining to the efforts aimed to prepare pure *c*-BN.

Experimental Section

Synthesis of BN nanoparticles

BN nanoparticles were synthesized according to the following process. Firstly, 10 g of BCl_3 was dissolved in 50 mL of redistilled benzene, and then 15 g of NaN_3 was added to the solution with stirring. After stirring for another 30 min, the resulting suspension was transferred into an autoclave with a teflon liner, and another portion of redistilled benzene was added to the autoclave to a filling ratio of 80%. The autoclave was then purged with pure nitrogen gas (99.999%) and sealed. In order to eliminate the influence of oxygen and moisture, all the above manipulations were performed in a glove box filled with nitrogen gas of high purity (99.999%). Finally, the autoclave was heated to 250 °C and held for 6 h.

When the autoclave was cooled down to r. t., the products were washed with acetone (3 times) followed by washing with deionized water (4 – 5 times). After being dried at 80 °C in vacuum for 8 h, the BN samples obtained were used as the starting material for the structural transformation experiments.

Structural transformation of BN nanoparticles in benzene

BN nanoparticles (0.15 g) were ground for 10 min and dispersed in 8 mL of redistilled benzene. The mixture was then treated in an ultrasonic horn for 5 min, and the resultant suspension was transferred into a hot-press autoclave (Fig. 9). A constant pressure applied on the autoclave was chosen within the range of 40 – 120 MPa, and the autoclave was then heated up to temperatures of 240 – 300 °C for 1 – 6 h. After the hot-press process was completed, the autoclave was let to cool down to r. t. under pressure. Releasing the pressure, a suspension was recovered and a dark-colored sample was obtained by filtering the suspension. The dark sample was redispersed in acetone and ultrasonically treated for 20 min. After separating the liquid by centrifugation (4000 rounds $\min^{-1}$), the sample was dried at 80 °C in vacuum for 8 h and then heated at 600 °C in a flow of pure nitrogen gas (99.999%) for 6 h to remove any residual organic material that may have been present. By changing temperature and pressure, a series of samples could be prepared through the above process.

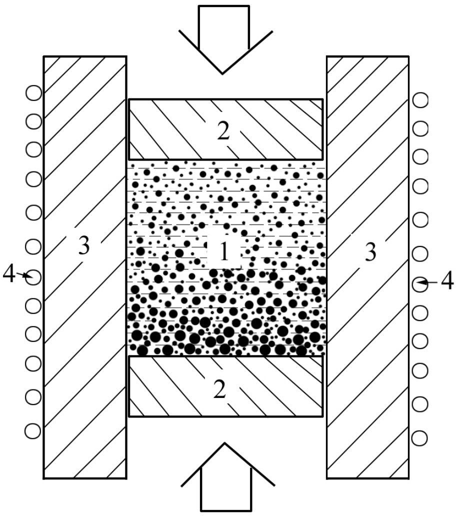

Fig. 9. Schematic structure of the hot-press autoclave. 1: benzene + BN nanoparticles; 2: piston; 3: cylinder; 4: heating coil.

Characterization of the samples

FTIR absorption spectra of the samples were collected on a Nicolet NEXUS 670 infrared spectrometer with the wave number resolution of 2 cm^{-1}. The morphology and selective area electron diffraction (SAED) patterns of BN particles were obtained using a Hitachi H-800 transmission electron microscope (TEM). The HRTEM images of the samples were observed on a Phillips Tecnai Twin-20U high resolution transmission electron microscope under an accelerating voltage of 200 kV.

Acknowledgements

The authors thank Prof. Jing Haipeng for helpful discussions and the correction of this manuscript. This work is supported by the National Natural Science Foundation of China (NSFC, No. 20473048, 90206042), Research Program of Ministry of Science and Technology (2005CCA00900), Science & Technology Research Program of Ministry of Education (No.104110, 305010) and Shandong Science and Technology Council (04BS04001, 2005GG3203110).

[1] R. Riedel, Adv. Mater. **6**, 549 (1994).

[2] P. B. Mirkarinmi, K. F. McCarty, D. L. Medlin, Mater. Sci. Eng. **47**, R21(1997).

[3] W. J. Zhang, I. Bello, Y. Lifshitz, S. T. Lee, MRS Bull. **184**, 28 (2003).

[4] O. Mishima, K. Era, J. Tanaka, S. Yamaoka, Appl. Phys. Lett. **962**, 53 (1988).

[5] L. Vel, G. Demazeau, J. Etourneau, Mater. Sci. Eng. B **149**, 10 (1991).

[6] R. H. Wentorf, J. Chem. Phys. **956**, 26 (1957).

[7] R. C. Devries, J. F. Fleischer, Mater. Res. Bull. **433**, 4(7) (1969).

[8] T. Endo, O. Fukunaga, M. Iwata, J. Mater. Sci. **1375**, 14 (1979).

[9] T. Sato, H. Hiraoka, T. Endo, O. Fukunaga, M. Iwata, J. Mater. Sci. **1829**, 16 (1981).

[10] T. Sato, T. Endo, S. Kashima, O. Fukunaga, M. Iwata, J. Mater. Sci. **3054**, 18 (1983).

[11] M. Kagamida, H. Kanda, M. Akaishi, A. Nukui, T. Osawa, S. Yamaoka, J. Cryst. Growth **261**, 94(1) (1989).

[12] V. L. Solozhenko, V. Z. Turkevich, Mater. Lett. **179**, 32 (1997).

[13] T. Taniguchi, S. Yamaoka, J. Cryst. Growth **549**, 222 (2001).

[14] K. Susa, T. Kobayashi, S. Taniguchi, Mater. Res. Bull. **1443**, 9 (1974).

[15] T. Kobayashi, J. Chem. Phys. **5898**, 70 (1979).

[16] T. Taniguchi, K. Kimoto, T. Masataka, S. Horiuchi, S. Yamaoka, Chem. Mater. **2744**, 15 (2003).

[17] J. Y. Huang, Y. T. Zhu, Chem. Mater. **1873**, 14 (2002).

[18] S. S. Batsanav, Q. E. Blokhina, A. A. Deribas, Zhurnal Strukturnoi Khimii **227**, 6 (1965).

[19] Z. Chen, Z. F. Lai, K. Li, D. L. Cui, N. Lun, Q. L. Wang, M. H. Jiang, Int. J. Modern Phys. B **2663**, 19(15–17) (2005).

[20] F. P. Bundy, R. H. Wentorf (Jr.), J. Chem. Phys. **1144**, 38(5) (1963).

[21] M. Ueno, K. Hasegawa, R. Oshima, A. Onodera, O. Shimomura, K. Takemura, H. Nakae, T. Matsuda, T. Hirai, Phys. Rev. B **10226**, 45(18) (1992).

[22] X. P. Hao, D. L. Cui, G. X. Shi, Y. Q. Yin, X. G. Xu, J. Y. Wang, M. H. Jiang, X. W. Xu, Y. P. Li, B. Q. Sun, Chem. Mater. **2457**, 13(8) (2001).

[23] A. Olszyna, J. Konwerska-Hrabowska, M. Lisicki, Diamond Relat. Mater. **617**, 6 (1997).

[24] H. Z. Zhang, B. Gilbert, F. Huang, J. F. Banfield, Nature **1025**, 424 (2003).

[25] L. L. Yu, B. Gao, Z. Chen, C. T. Sun, D. L. Cui, C. J. Wang, Q. L. Wang, M. H. Jiang, Chin. Sci. Bull. **2827**, 50(24) (2005).

[26] P. B. Mirkarimi, K. F. McCarty, D. L. Medlin, W. G. Wolf, T. A. Friedmann, E. J. Klaus, G. F. Cardinale, D. G. Howitt, J. Mater. Res. **2925**, 9 (1994).